



INSTITUT DE FRANCE
Académie des sciences

Comptes Rendus

Mécanique


Luis Carlos Martínez-Mendoza, Florencio Sánchez-Silva, Erik Fernando Martínez-Mendoza and Juan Antonio Cruz-Maya

Numerical study of fluid flow at pore scale in packed bed of spheres and grains to obtain the REV

Volume 348, issue 8-9 (2020), p. 769-779.

<<https://doi.org/10.5802/crmeca.62>>

© Académie des sciences, Paris and the authors, 2020.
Some rights reserved.

 This article is licensed under the
CREATIVE COMMONS ATTRIBUTION 4.0 INTERNATIONAL LICENSE.
<http://creativecommons.org/licenses/by/4.0/>



Les Comptes Rendus. Mécanique sont membres du
Centre Mersenne pour l'édition scientifique ouverte
www.centre-mersenne.org



short paper / note

Numerical study of fluid flow at pore scale in packed bed of spheres and grains to obtain the REV

Luis Carlos Martínez-Mendoza^{*, a}, Florencio Sánchez-Silva^a,
Erik Fernando Martínez-Mendoza^a and Juan Antonio Cruz-Maya^b

^a Laboratorio de Ingeniería Térmica e Hidráulica Aplicada, ESIME, Unidad Profesional Adolfo López Mateos, IPN, Col. Zacatenco, Ciudad de México, 07738, México

^b Unidad Profesional Interdisciplinaria en Ingeniería y Tecnologías Avanzadas, IPN, Av. IPN 2580, Col. La Laguna Ticomán, Ciudad de México, 07340, México

E-mails: lmartinezm1308@alumno.ipn.mx (L. C. Martínez-Mendoza), snchz@yahoo.com.mx (F. Sánchez-Silva), erikfermm@hotmail.com (E. F. Martínez-Mendoza), jacm.maya@gmail.com (J. A. Cruz-Maya)

Abstract. This paper presents a numerical study to determine the Representative Elemental Volume (REV) size of a porous medium made of packed bed of non-deformable spheres and grains with morphology of Berea sandstone, by means of stochastic packing methods. The Navier–Stokes equations and CFD simulations at the pore level are used to calculate the macroscopic properties of the porous media, such as overall permeability, porosity, and tortuosity. The results obtained show that the values of these parameters present an asymptotic behavior, in the limit values of the REV. This allowed to establish a minimum size of REV, in which it is suggested to carry out the flow analyses to optimize the cost of computational resources without sacrificing the precision of the results.

Keywords. Permeability, CFD, Porous media, REV, Numerical simulation.

Manuscript received 8th May 2020, revised 16th November 2020, accepted 17th November 2020.

1. Introduction

From the pharmaceutical industry, the food industry, to the extractive industry, it is necessary to determine the relationships existing between the different physical parameters that define the morphology and macroscopic properties of the porous media. Today, the Digital Rock Physics (DRP) has taken on a relevant importance for the study of phenomena transport in porous

* Corresponding author.

media and the main element of this approach is the numerical simulation at the pore level. However, due to the complexity and morphological variability of the porous media at the pore level, robust numerical schemes are required for its study. Therefore, for this branch of study it is of great interest to determine an optimal computational domain, which allows a reliable numerical simulation with the minimum computational effort.

Most of the numerical studies are carried out considering the porous media as a homogeneous medium, without considering its particular morphology found within it [1]. It is also assumed that macroscopic properties, such as permeability and porosity, can be described by microscopic parameters related to the particles of the porous medium, such as size, shape, sorting, and cementation. The morphology of the porous media and the inertial effects at the pore scale has an important influence to improve the numerical results precision. Recent developments in pore scale modeling, coupled with the specialization of imaging techniques [2, 3], have allowed direct numerical simulations of fluid flow through intricate microscopic structures to be developed [4]. The direct modeling approach, in which the fundamental equations of flow and transport are solved in the real geometry of the pore space, is very precise; however, it has a great computational cost. The results obtained in the microscale numerical analyses can be integrated into continuous scale models, which are then used to support decision making (at the field scale) in the management of oil, gas, and water fields underground [4]. In addition, this topic is of great interest for the numerical characterization of fluid mobility in rock reservoir, during Enhance Oil Recovery (EOR) processes. In these process, several fluids are injected, such as, foam, steam, CO₂, etc., in order to promote oil recovery mechanisms.

Traditionally, fluid flow in porous rock is commonly investigated by physical core flooding experiments. To perform these tests, a core-plug of natural rock is placed in a core support (core-holder), which is a pressure vessel, subject to high confining pressure, through which fluids circulate. However, the numerical study of macroscopic properties in a complete core-plug would require a numerical domain with a very high computational cost, due to the large number of particles and the geometric definition of the pore network.

The interest of this study is to determine a Representative Elemental Volume (REV) in a general porous medium and in porous core-plug samples, made of conglomerates of spherical particles and grains with Berea sandstone morphology. Traditionally, particles with spherical geometry have been used to represent porous media [5–7]. The petroleum industry has been using Berea sandstone, as the material of choice to represent reservoir rock, in experimental tests. The REV, then, will be defined as the minimum computational volume to obtain reliable numerical results with low computational cost. Obtaining the REV will allow to work at a reliable macroscopic scale to core-flood numerical experiments, by means of Computational Fluid Dynamics (CFD).

Representative Elemental Volume (REV) is defined as the minimum scale, at which macroscopic parameters, such as permeability, porosity, and tortuosity do not depend of the heterogeneities at the microscopic level [8]. Figure 1 shows the schematic representation of the REV in which the macroscopic properties such as porosity of the porous media tend to remain constant throughout of the length sample. Several studies have been carried out to obtain the REV, using numerical simulations by Lattice–Boltzmann method [5, 9, 10], and employing laboratory tests [11, 12]. This work focuses on obtaining the REV in digital core-plugs, by means of the behavior of the macroscopic parameters of permeability, porosity, and tortuosity of the porous medium, using CFD techniques with open-source platform OpenFOAM® [13].

2. Development proposal

To obtain the REV, basically, it consists of determining a sufficient length L of the computational domain, along the flow direction in the porous medium, in which the values of the macroscopic

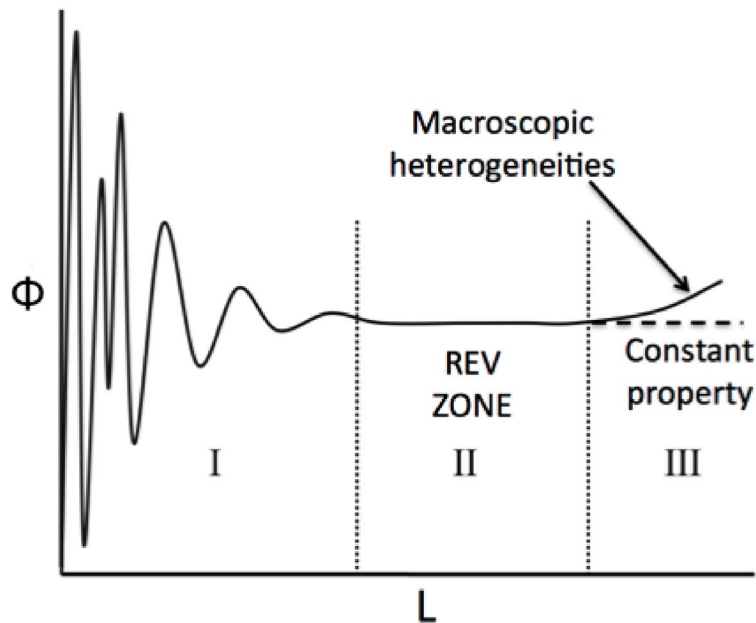


Figure 1. Schematic representation of the REV by means of the porosity behavior in the sample length L [8].



Figure 2. Digital transition of the particles used in the digital packings, from digital reconstruction of Berea sandstone grain to a spherical particle.

properties and characteristics of the porous media, such as permeability, porosity, and tortuosity are independent of the length L of the porous media. The length L of the porous media can be normalized with respect to some geometrical parameters that denote the average size of the micro-heterogeneity of the porous media, such as volume-equivalent diameter D of the particle (sphere or grain), to define the dimensionless length (L/D), where, L denotes a mesoscale domain and D denotes the microscale domain of the porous media.

The digital samples of porous media used in the present study were constructed using an object oriented programming technique by means of open-source software YADE-OPEN DEM [14], which employs a Discrete Element Method (DEM), to simulate compaction of powders and granular material by means of the stochastic methods. The REV analysis was based on the pressure and flow velocity profiles, obtained from the numerical simulation of the flow at the pore level, carried out on eight digital porous samples, defined in the Table 1. The particles used in digital packing were rigid spheres and digitized Berea sandstone grains with a realistic morphology from the tomographic study. Figure 2 shows the geometric transition of the particles used in digital packaging, from a digital reconstruction of Berea sandstone grain to a spherical particle. During digital construction of samples, morphological parameters of the particles, such as size

Table 1. Results obtained for permeability, tortuosity, and porosity for the computational domain (L/D) for which the REV starts

Case	Particle geometry	aVED [†] (μm)	L/D [‡] REV	K (3) Darcy	τ	ϕ	K (KC) (9) Darcy
1	Mono-sized spheres	10	10	0.252	1.2	0.475	0.213
2	Mono-sized spheres	50	10	3.546	1.197	0.43	3.361
3	Mono-sized spheres	60	10	5.107	1.189	0.428	4.749
4	Mono-sized grains	42.72	15	2.650	1.248	0.429	2.423
5	Multi-sized grains	42.12	15	2.494	1.261	0.415	2.043
6	Multi-sized grains	40.2	15	1.544	1.313	0.396	1.521
7	Mono-sized grains with reduction poral space	42.72	15	1.797	1.332	0.376	1.372
8	Mono-sized grains with extreme reduction poral space	42.72	15	0.0716	1.814	0.147	0.043

[†] average Volume-Equivalent Diameter (aVED), was used to define the average diameter D of the packing sample.

[‡] Dimensionless length L/D , for which the REV starts.

and shape, in addition to pore space of the samples, were manipulated, in order to obtain representative cases studies, with dispersion in the values of the macroscopic parameters (permeability, porosity, and tortuosity) of the samples. Figure 3 shows the packings built of spheres and grains, to case studies 1 and 5, respectively. The advantage of constructing packings digitally is based on the morphological manipulation of the samples to develop specific samples ad hoc to the numerical study.

2.1. Porosity determination

For the oil extraction industry, porosity (ϕ) is considered one of the most important properties of the porous media since it is a measure of the space available for the storage of hydrocarbons. Porosity, is defined as the fraction of the total volume (V_T) that is occupied by the empty spaces or poral volume (V_P). These values are obtained directly during the digital built of the packing porous samples.

$$\phi = \frac{V_P}{V_T}. \quad (1)$$

2.2. Permeability prediction

Another important property of porous media is its permeability, which represents the ability of the porous material to allow fluid flow. In this regard, it is a very important property of the porous medium, since it controls the direction of flow and its velocity in the reservoirs. One of the simplest correlations and one that has shown good results is Darcy's law [15]:

$$k_{ij} = -\frac{\mu}{\nabla P_j} \langle v_i \rangle, \quad (2)$$

where $\langle v_i \rangle$ is the velocity in the i direction averaged over the control volume, μ is the dynamic viscosity of the fluid, ∇P is the pressure gradient in the j direction, and k_{ij} is the permeability tensor. This tensor is normally diagonal and positive, its elements can be determined using

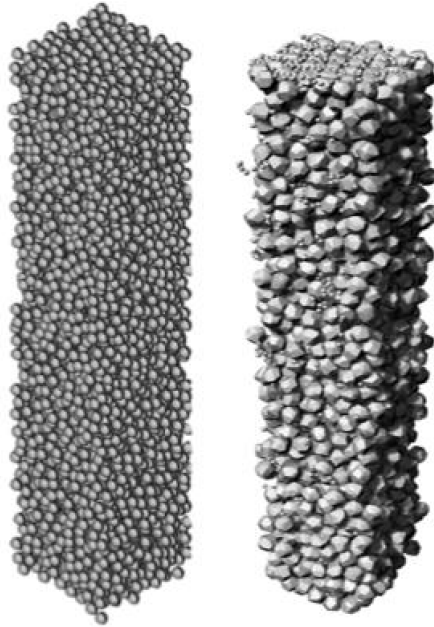


Figure 3. Scale packings, built for case studies 1 and 5, (a) spheres, (b) Berea sandstone grains, respectively.

experimental [16] and numerical simulation results [4]. Permeability is calculated from the applied pressure gradient ΔP and the length of the system in the main flow direction over which the pressure gradient has been imposed, for a given single-phase flow, with a known and constant viscosity. Darcy's law is valid for low velocity flows of a Newtonian fluid through a porous medium, where inertial effects can be neglected [6]. Several investigations have been carried out which have determined that the permeability depends directly on the porosity of the porous medium and varies with the internal structure of the material [17, 18]. To determine permeability, from Darcy's law (3), we consider the applied pressure gradient ∇P and the velocity vector v in the main flow direction, which are determined from pressure distribution and velocity profile obtained of the numerical simulation, respectively.

$$k_{ij} = -\frac{\mu}{\nabla P} \left(\frac{1}{V} \int v_i dV \right). \quad (3)$$

2.3. Tortuosity calculation

Tortuosity (τ) is defined as the ratio between the actual path length followed by the flow within the poral network, defined as L_p and the linear distance through the porous medium in the direction of the macroscopic flow L_0 ; therefore, it is always greater than the unit [7]:

$$\tau = \frac{L_p}{L_0} \geq 1. \quad (4)$$

There are different ways of calculating this parameter, which have been developed for packing of different particle geometries [19]. As a result, different correlations have been obtained for the calculus of the tortuosity, which are conditioned to the specific geometry of the particle [20]. Furthermore, there are several numerical technics [21] capable of adapting to complex geometries of the pore space, for the calculation of tortuosity. However, they require a lot of computational

effort. A consistent and simple way to determine the tortuosity is proposed by Carman [21], using the relationship defined by

$$\tau = \frac{\langle v_T \rangle}{\langle v_z \rangle}, \quad (5)$$

where $\langle v_T \rangle$ and $\langle v_z \rangle$ are the velocity averaged in the control volume and the velocity in the direction of the macroscopic flow, respectively. The velocity values are determined by means of the velocity profiles of the numerical simulation. Its main advantage is to allow the calculation of tortuosity without needs to determine individual streamlines [21].

3. Numerical simulation overview

3.1. Fluid flow equations in porous media

The velocity and pressure profiles of the fluid flowing through the poral space of the sample cases, can be obtained by solving the mass and momentum equations, equations (6) and (7), respectively.

$$\nabla \cdot \mathbf{u} = 0 \quad (6)$$

$$\frac{\partial \mathbf{u}}{\partial t} + \mathbf{u} \nabla \cdot \mathbf{u} = -\frac{\partial p}{\partial \mathbf{x}} + \nu \nabla^2 \mathbf{u}, \quad (7)$$

where ν the kinematic viscosity, \mathbf{u} the velocity vector, and p is pressure. The governing equations of the computational domain in study, such as core-plug samples, can be reduced to Stokes' equation, considering laminar flow regimes and small inertial forces, compared to viscous forces. Therefore, equation (7) can be expressed by

$$\frac{\partial p}{\partial \mathbf{x}} = \nu \nabla^2 \mathbf{u}. \quad (8)$$

3.2. General numerical simulation conditions

- Rigid and non-deformable spheres and grains with morphology of Berea sandstone, which do not interact with fluid flow.
- 3D computational domain with dimensions in the x , y , and z coordinates, with a dimensionless length L/D of $5 \times 5 \times 1.25$ (minimum domain) to $5 \times 5 \times 30$ (overall domain).
- Steady and laminar flow with isothermal condition.
- Continuous, Newtonian and incompressible flow.
- To packings of Berea sandstone grains, was used the volume-equivalent diameter, in order to define the equivalent diameter D of the grain in the dimensionless length L/D . The volume-equivalent diameter D is defined as the diameter for the sphere with the same volume as the particle.

During the numerical simulation of the flow, the pressure gradient is parallel to the axis of the porous media (core-plug) and the volumetric flux would then be exactly the flow rate per cross-sectional area of the core-plug perpendicular to axis of the core, in which the component of the flow rate vector is parallel to the core axis. In this case, the orientations of the pressure gradient and the filter velocity are the same. Therefore, the component of interest in the permeability tensor of the core-plug is reduced to direction of the core axis.

SnappyHexMesh OpenFOAM[®] was used in the mesh generation process, which generates 3-dimensional meshes containing hexahedra (hex) and split-hexahedra (split-hex) elements automatically from triangulated surface geometries, in STereoLithography (STL). The numerical simulations were carried out using OpenFOAM7.0 CFD software, which is based on the finite volume approach for the discretization of the governing equations. The coupling between the

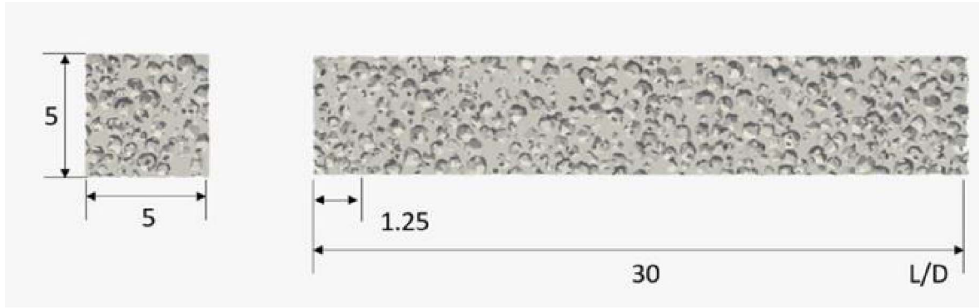


Figure 4. Computational domain selected to simulation cases 1 to 8. The minimum computational domain was with a ratio of the sample porous length L to particle diameter D of $5 \times 5 \times 1.25$ (L/D) to overall domain of $5 \times 5 \times 30$ (L/D).

Table 2. Numerical simulation boundary conditions

Boundary	Condition
Inlet	Inlet pressure
Outlet	P of output 0 (Pa)
Boundaries of control volume	Symmetry
Grain surface	No slip

pressure and velocity equations is achieved using the semi-implicit method for pressure linked equations (SIMPLE) algorithm. The boundary conditions used during the numerical simulation for case studies 1–8 are defined in Table 2. The minimum computational domain used in the case studies 1 to 8 was with a ratio of the sample porous length L to particle diameter D of $5 \times 5 \times 1.25$ (L/D). The computational domain was systematically increased through the length of the sample in the flow direction to overall domain of $5 \times 5 \times 30$ (L/D), in order to observe the variability of the permeability, porosity, and tortuosity values. Figure 4 shows a computational domain selected to simulation cases 1 to 8.

4. Results

The determination of REV is based on achieving the asymptotic behavior of the macroscopic variables permeability, porosity, and tortuosity in a certain computational domain, where the heterogeneity of the porous medium at the microscale level is not significant in the variability of these parameters, as shown in Figure 1.

We now present the values obtained for porosity, permeability, and tortuosity by means of equations (1), (2), and (5), respectively. These equations were fed with the numerical results of the pressure distribution and the velocity field of eight cases study, defined in Table 1. Figure 5 shows the velocity field and the pressure distribution, obtained from the numerical simulation of case study number 6. The study cases considered 120 points of numerical simulation, in which the morphological parameters were systematically varied in the built samples, such as the size and shape of the particle, in addition to the poral space. The variability in the morphological parameters was used to cover a wide range of permeability, porosity, and tortuosity results, which allowed the identification of REV for a wide variety of conditions. The permeability results are shown in a dimensionless way, taking the volume-equivalent diameter of the particle D , as a microscopic reference, to establish dimensionless permeability K_{adim} as the K/D^2 ratio. Figure 6 shows the variation of the dimensionless permeability K_{adim} in dimensionless length L/D of the

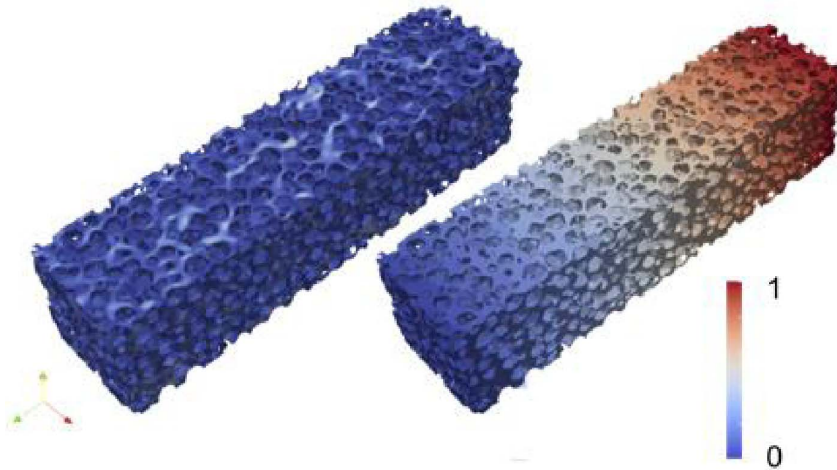


Figure 5. Velocity field (left) and pressure distribution (right) from numerical simulation for case study number 6.

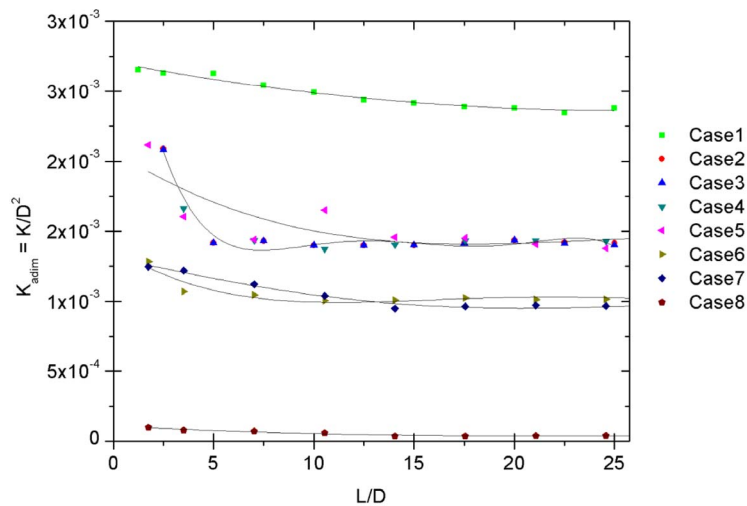


Figure 6. Variations in dimensionless permeability K_{adim} versus dimensionless length L/D for case studies 1 to 8.

porous sample. The results obtained show a strong variability of the dimensionless permeability (K_{adim}) for the computational domain less than $L/D = 10$, in all the study cases. In the vicinity of this limit ($L/D = 10$), the behavior of K_{adim} for packings of spherical particles (cases 1–3), tends to behave in an asymptotic way, indicating the independence of the relationship L/D and the beginning of the lower limit of the REV. To cases 4–8 of porous samples with sandstone grain morphology, the shape and size grains effects and reducing poral network size delayed the asymptotic behavior of permeability K_{adim} , along the length of the sample, which is accentuated in the vicinity of $L/D = 15$.

Figure 7 shows the values obtained for the tortuosity of cases 1 to 8, versus dimensionless length L/D . It is observed at the limit of $L/D = 10$, the beginning of an asymptotic behavior of the tortuosity, for cases 1–3 corresponding to porous samples of spheres. For porous grain

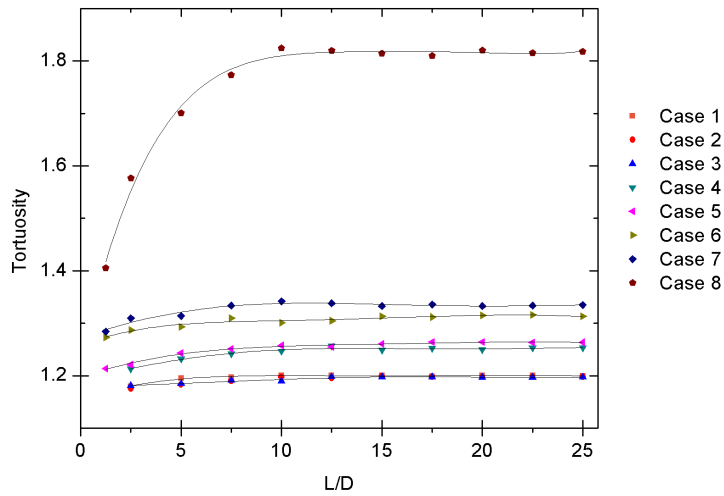


Figure 7. Tortuosity behavior in dimensionless length L/D for case studies 1 to 8.

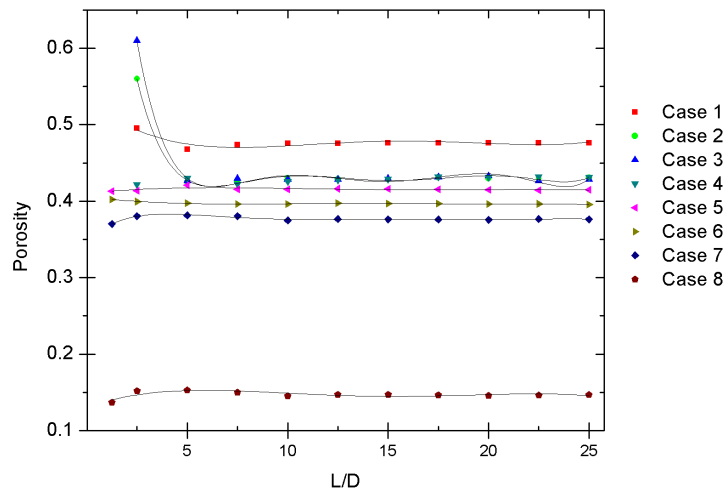


Figure 8. Porosity versus dimensionless length L/D for case studies 1 to 8.

samples (cases 4–8), the tortuosity becomes independent of the microscopic effects when it approaches a length ratio of $L/D = 15$. The asymptotic behavior of the tortuosity is similar to that shown by the permeability. In the cases 7 and 8, the reduction of the pore space was digitally manipulated, simulating a diagenesis process, which occurs as a result of various chemical and biological processes that lead to erosion, as well as the formation of mineral deposits or cementation in the poral space of the real rocks. To reproduce this phenomenon digitally, the sedimentation algorithms were completed with a geometric cementation algorithm using FreeCAD software [22], in order to simulate the alteration of the pore space by diagenesis. As a result of the alteration of the poral space, the tortuosity showed a strong variability for $L/D < 15$. However, it did not alter the behavior of the tortuosity for values greater than $L/D = 15$, so the onset of the REV occurs in the same computational domain as the other study cases. Porosity shows an asymptotic behavior for the L/D ratio > 15 , for all cases, as shown in Figure 8.

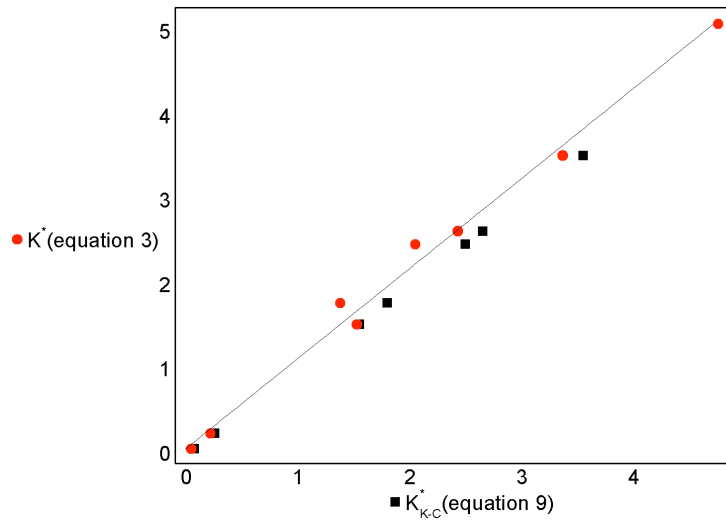


Figure 9. Dimensionless permeability K^* (equation (3)) data versus the dimensionless $K-C^*$ predicted permeability (equation (9)).

We observe that the REV practically becomes insensitive to the variation in the morphological parameters at microscale of the porous samples and to the variation in the calculus of the macroscopic properties (less 3%), for computational domains greater than dimensionless length $L/D = 15$. Therefore, we can define the limit of the REV, for a computational domain in the flow direction, equal to $L/D = 10$ in the case spheres (cases 1–3) and $L/D = 15$ for grain packings (cases 4–8). Table 1 shows the results obtained for permeability, tortuosity, and porosity for the computational domain (L/D) for which the REV starts. The results obtained for permeability by means of equation (3) are compared against the Kozeny–Carman (KC) equation (9), which is taken as a comparison reference. The results show a good concordance in the cases 1–6 as shown in Figure 9. The difference between the permeability values calculated numerically using equation (3) and the values determined using Kozeny–Carman equation (9) [23] is more notable in cases 7 and 8 (Table 1). In these cases, the pore space was reduced drastically altering the morphology of the porous medium.

$$k = \frac{d^2 \phi^3}{36 c \tau^2 (1 - \phi)^2}, \quad (9)$$

where $c \tau^2$ is the KC empirical constant and τ is the tortuosity. The empirical KC constant is approximated to be 5, for beds packed with spherical particles.

5. Conclusions

The numerical calculus of the macroscopic properties of the porous medium, such as porosity and permeability, are significantly affected by the size of the computational domain. This situation makes it necessary to delimit a representative REV of the porous sample, in order to carry out numerical studies with reliability, without great computational effort.

The OpenFOAM7.0 CFD was used to simulate Stokes flow at the pore scale in artificially built porous media, with spherical particles and grains with Berea sandstone morphology, using open-source software YADE-OPEN DEM. This allowed the determination of the computational domain of the REV, considering the complex morphology of the porous medium, such as the

rock reservoir. The packaging of particles, using YADE-OPEN DEM, allowed to manipulate the morphological characteristics of the porous samples, such as particle size and shape, as well as pore space. This situation allowed the construction of specific porous samples with reservoir rock morphology (core-plugs), to study the effect of several parameters in the REV determination. The core-plugs are used for the experimental study of macroscopic properties and fluid mobility studies in core flooding tests. The numerical study of the flow at pore scale, in the built samples, allowed to delimit a computational domain, in which the microscopic effects related to the morphology of the porous media, such as the shape and size of the particles, sorting, and poral space, were independent of variables such as permeability, porosity, and tortuosity, to determine the REV.

References

- [1] W. G. Gray, C. T. Miller, "Examination of Darcy's law for flow in porous media with variable porosity", *Environ. Sci. Technol.* **38** (2004), no. 22, p. 5895-5901.
- [2] N. O. Shanti, V. W. L. Chan, S. R. Stock, F. De Carlo, K. Thornton, K. T. Faber, "X-ray micro-computed tomography and tortuosity calculations of percolating pore networks", *Acta Mater.* **71** (2014), p. 126-135.
- [3] D. Wildenschild, A. P. Sheppard, "X-ray imaging and analysis techniques for quantifying pore-scale structure and processes in subsurface porous medium systems", *Adv. Water Resour.* **51** (2013), p. 217-246.
- [4] M. Siena *et al.*, "Direct numerical simulation of fully saturated flow in natural porous media at the pore scale: a comparison of three computational systems", *Comput. Geosci.* **19** (2015), no. 2, p. 423-437.
- [5] P. Wang, "Lattice Boltzmann simulation of permeability and tortuosity for flow through dense porous media", *Math. Probl. Eng.* **2014** (2014), p. 1-7.
- [6] D. Pavlidis, D. Lathouwers, "Realistic packed bed generation using small numbers of spheres", *Nucl. Eng. Des.* **263** (2013), p. 172-178.
- [7] W. Sobieski, "The use of Path Tracking Method for determining the tortuosity field in a porous bed", *Granul. Matter* **18** (2016), no. 3, p. 1-9.
- [8] J. Bear, *Dynamics of Fluids In Porous Media, Vol. 1*, American Elsevier Publishing Company, 1972.
- [9] D. Zhang, R. Zhang, S. Chen, W. E. Soll, "Pore scale study of flow in porous media: scale dependency, REV, and statistical REV", *Geophys. Res. Lett.* **27** (2000), no. 8, p. 1195-1198.
- [10] C. Yuan, B. Chareyre, F. Darve, "Pore-scale simulations of drainage in granular materials: Finite size effects and the representative elementary volume", *Adv. Water Resour.* **95** (2016), p. 109-124.
- [11] G. O. Brown, H. T. Hsieh, D. A. Lucero, "Evaluation of laboratory dolomite core sample size using representative elementary volume concepts", *Water Resour. Res.* **36** (2000), p. 1199-1207.
- [12] B. Vik, E. Bastesen, A. Skauge, "Evaluation of representative elementary volume for a vuggy carbonate rock-Part: Porosity, permeability, and dispersivity", *J. Pet. Sci. Eng.* **112** (2013), p. 36-47.
- [13] H. G. Weller, G. Tabor, H. Jasak, C. Fureby, "A tensorial approach to computational continuum mechanics using object-oriented techniques", *Comput. Phys.* **12** (1998), no. 6, p. 620-631.
- [14] V. Šmilauer *et al.*, "Yade Documentation", 2015, 2nd edition, software documentation of Yade-DEM with some theoretical background.
- [15] G. O. Brown, "Henry Darcy and the making of a law", *Water Resour. Res.* **38** (2002), no. 7, p. 11-1-11-12.
- [16] L. Luquot, P. Gouze, "Experimental determination of porosity and permeability changes induced by injection of CO₂ into carbonate rocks", *Chem. Geol.* **265** (2009), no. 1-2, p. 148-159.
- [17] V. M. Starov, V. G. Zhdanov, "Effective viscosity and permeability of porous media", *Colloids Surf. A* **192** (2001), p. 363-375.
- [18] S. Whitaker, "Flow in porous media I: A theoretical derivation of Darcy's law", *Transp. Porous Media* **1** (1986), no. 1, p. 3-25.
- [19] B. Ghanbarian, A. G. Hunt, R. P. Ewing, M. Sahimi, "Tortuosity in porous media: a critical review", *Soil Sci. Soc. Am. J.* **77** (2013), no. 5, p. 1461-1477.
- [20] W. Sobieski, S. Lipiński, "The analysis of the relations between porosity and tortuosity in granular beds", *Tech. Sci.* **20** (2017), no. 1, p. 75-85.
- [21] A. Duda, Z. Koza, M. Matyka, "Hydraulic tortuosity in arbitrary porous media flow", *Phys. Rev. E* **84** (2011), no. 3, p. 1-8.
- [22] J. Riege, W. Mayer, Y. van Havre, "FreeCAD", 2019 (Version 0.18) [Software], available from <http://www.freecadweb.org>.
- [23] M. M. Ahmadi, S. Mohammadi, A. N. Hayati, "Analytical derivation of tortuosity and permeability of monosized spheres: A volume averaging approach", *Phys. Rev. E* **83** (2011), no. 2, p. 1-8.